

Ultrasonic Elastogram Generation by 2D Thin Plate Smoothing Spline based Mathematical Interpolation Technique

Safayat Bin Hakim

Islamic University of Technology
Department of Electrical & Electronic Engineering
Gazipur-1704, Dhaka
Bangladesh.

Kazi Khairul Islam

Islamic University of Technology
Department of Electrical & Electronic Engineering
Gazipur-1704, Dhaka
Bangladesh.

ABSTRACT

Use of mathematical interpolation in Digital Signal Processing applications often seems to be a remarkable solution when applied for noise reduction. In the last two decades advancement in the Elasticity imaging of tissue is worth mentioning. Two dimensional spline technique for generating Elastograms is fairly a new approach for generating ultrasonic Elastograms. In the way of analyzing imaging modalities generally three parameters are taken into account resolution, SNR_e and CNR_e . In ultrasound elastography spline based method for axial strain estimation is well-established in the literature. In this paper we have shown the possibilities of 2D spline which mainly works on a plate of experimental data considering both axial and the lateral directions. We have also analyzed the improvement of performance while utilizing this method comparing with other well-established techniques such as simple *1D Smoothing Spline* and the *Adaptive Strain Estimation* technique.

Keywords:

Strain estimation, Smoothing spline, Resolution, Performance parameter, Interpolation.

1. INTRODUCTION

Research of non-invasive techniques are always a center of attraction for the researchers all over the world. Elastographic technique added a new dimension in this arena for detecting deep-lying suspected nodules in human body. The term Elastography was first coined by Ophir *et.al* in a paper published in 1991 [1]. Now this is a well-established and well-exercised technique for effective discrimination of biological tissue pathology change in medical diagnosis. Pathological state has correlation with the changes in tissue elasticity [2] [3]. Strain Imaging is mainly measuring the local tissue deformation which is a resultant of stress applied mechanically. Mechanical properties which are the actual desired information in this process retrieved by the way in which the tissue deforms [4] [5]. The local axial displacements are then calculated by estimating the time delay between the corresponding segments of the pre and post-compression RF signals. Finally, the local axial strains are calculated as the gradient of the axial displacements and the elastogram (strain image) is generated [6]. An ideal strain estimator has to generate the elastograms with high SNR_e , CNR_e , spatial resolution and also should be as time efficient as possible [7]. The time efficiency of

a technique makes it capable of being used in real time applications.

The most widely used statistical spatial filters to reduce the noise are Min, Max, Mean, Median, Midpoint, M3, Harmonic Mean, Contra Harmonic Mean and Geometric Mean [8]. There exists a handsome number of proposition for reconstructing elastograms or strain images which are mainly axial deformation based one dimensional (1D) cross-correlation methods applied to the radio frequency (RF) [9] [10] ultrasonic echoes backscattered by tissue scatterers pre and post compression [11]. An inevitable trade-off in case of these several techniques is time efficiency and the improved performance parameters [12] [13]. That means time efficient algorithms are burdened with lower value of SNR_e and CNR_e . In the contrary algorithms which provides high accuracy strain estimation with high SNR_e and CNR_e are unable to compensate a bulk amount of time to be implemented. An ideal strain estimator has to generate the elastograms with high SNR_e , CNR_e , spatial resolution and as well as time efficient as possible [14][15]. The time efficiency of a technique makes it capable of being used in real time applications.

2. 2D THIN PLATE SMOOTHING SPLINE TECHNIQUE

Curve fitting from a set of point needs to follow an unique interpolation technique. There are several methods *e.g.* Linear, Cubic, Parabolic, Lagrange, Cosine, Hermite, Shape preserving, Nearest neighbour *etc.* Spline is a piecewise polynomial interpolation [16]. Curve fitting using spline based approach gives high degree smoothness at the places where the polynomial pieces connect. In other words smoothing noisy data values observed at n distinct points on a finite interval [17].

Thin plate smoothing spline (TPSS) is mainly 2D generalization of Cubic spline [18]. To fit a thin plate spline to n data requires the estimation of n parameters and an additional smoothing parameter. TPSS is extensively used in 3D Image Recovery, finger print analysis, image warping, modelling coordinate transformation, medical Image Analysis, data mining [19]. It comes mainly from the interpolation technique. In a precise mathematical description it is mainly a sort of numerical analysis of constructing new data points within the range of a discrete set of known data points. In other words estimating a continuous function by another continuous function [20]. There are a lot of interpolation

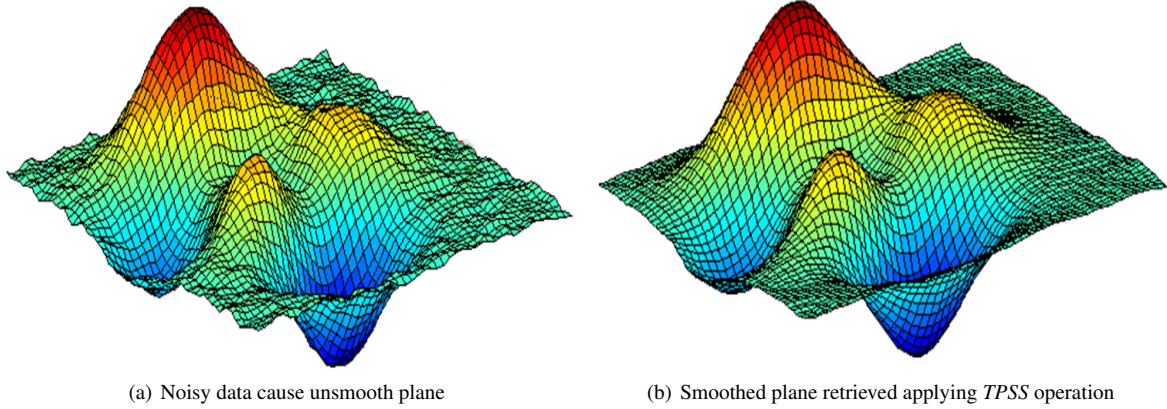


Fig. 1. Generating smooth plane applying 2D Thin Plate Smoothing Spline (TPSS) operation on the first figure.

technique exists such as cubic, spline, linear, hermite, cosine *etc.* As we know that if we take a curve according to the displacement of a fixed interval at every consecutive times after the use of controlled strain source which is an ultrasound transducer in our case as an obvious reason; upon a soft biological tissue the shape of that displacement curve does not change rapidly. Utilizing that fact it is possible to fit a suitable smooth curve through the estimated displacements and consider the derivative of the resulting continuous function as the corresponding continuous axial strain profile. We know that gradient operation on displacement values is a fundamental step before generating Elastogram [21]. In our experiment gradient operation is still the last step but we are optimizing our displacement data by 2D smoothing spline operation. After completion of these steps we will apply gradient operation.

Let us assume a noisy displacement function χ . Now piecewise polynomial based smoothing spline algorithm performs an interpolation which eventually mitigates the noisy environment and the algorithm works on the overall $(\chi_\eta, \lambda_\eta)$ points :

$$\rho \sum_{\eta=1}^m w(\eta) |\gamma[\chi(\eta)] - \zeta[\chi(\eta)]|^2 + (1-\rho) \int_{\min(x)}^{\max(x)} \lambda(t) |D^\varepsilon \zeta(t)| dt \quad (1)$$

The smoothing spline ζ is constructed for the specified smoothing parameter ρ ($0 \leq \rho \leq 1$) and the specified weights w_η [22]. ζ is a piecewise, three times differentiable, cubic polynomial. Strain is estimated by computing the gradient of the smoothing spline ζ . χ is the data site; γ is the data value; λ is the piecewise constant weight function and D^ε represents the ε^{th} derivative.

Equation -1 works fine for one-dimensional spline interpolation. But for thin plate spline it is needed to modify the mathematics so that it can take into account both the dimensions in single mathematical interpretation. *TPS* is 2D interpolation which represents a simple thin metal sheet and the sheet is formed in such a way that it is limited to move at the grid points. The metal sheet is also free from any external force relied upon control points [23]. The metal sheet is also free from any external force relied upon control points. The *TPS* model describes the transformed coordinates (x', y') both independently as a function of original coordinates (x, y) :

$$x' = f_x(x, y) \quad (2)$$

$$y' = f_y(x, y) \quad (3)$$

Landmark points are those primordial points directly from two dimensional data table. When *TPS* model interpolates those points then there are displacements from the original location while ensuring the maximal smoothness. The smoothness is represented by the bending energy of the thin metal plate. Considering the 2^{nd} order partial derivatives over the entire surface “bending energy” can be retrieved and utilizing the solution of a set of linear equations it can be minimized [24]. In the following equation one of the transformed coordinates is given by parameter vectors ϑ and \aleph (using *TPS* model) :

$$f(x, y) = \vartheta_1 + \vartheta_2 x + \vartheta_3 y + \sum_{j=1}^m \aleph_j \prod_i (|\psi_j - (x, y)|) \quad (4)$$

where $\prod_i(\varrho) = \varrho^2 \log(\varrho)$ is the basis function, ϑ is responsible for transformation, \aleph gives an additional non-linear deformation ψ_j are the landmarks that the *TPS* interpolates, and m is the number of landmarks [25].

3. MATERIALS AND METHODS

We have used the Finite Element Model Analysis simulation phantom for checking the performance of different salient features of the proposed methods. A rectangular phantom of $20mm \times 20mm$ was simulated using the software named *Algor* (*Algor, Inc.*, Pittsburgh, PA) by FEM method. It has a homogeneous background with the stiffness of 60 kPa with two circular inclusions. We have chosen 60 kPa as stiffness because it is close to the average stiffness of normal glandular tissue in the breast [26][27]. Both the circular inclusions are 7.5 millimetre (*mm*) in diameter which is embedded in the phantom.

The stiffness of these four inclusions are also different from each other; top inclusion is +10 dB (10 times) and the bottom inclusion is +40 dB (10,000 times) stiffer than their background. The bottom of the phantom was placed on a planar surface and the phantom was in full free-slip condition (allowed to expand) at top and bottom surfaces. During the simulation, the Poisson’s ratio was used as 0.495. The phantom was compressed from the top using a larger-width planar compressor.

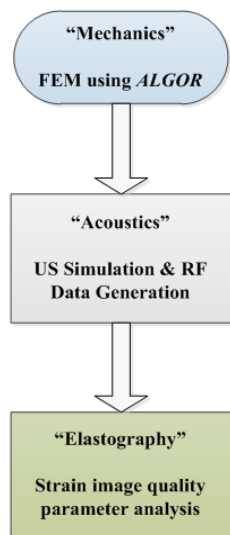


Fig. 2. Generalized block diagram representation of the major steps that comprise the simulation procedure.

An ultrasonic transducer was used to scan the phantom from the top (center frequency, $f_c=5$ MHz, band-width = 60%). A non-diffracting transducer beam was simulated with a beam width of 1.5 mm. The total number of A-lines was 128. Random white noise was added to simulate a sonographic SNR of 40 dB. Despite the uniform stiffness background, the strain variations occur in the back ground region due to interaction between lesions. With the increase of the percentage applied strain there will be distortion which is sometimes almost random in case of the inclusions compared to their background. For the numerical analysis and all kinds of computation was done using MATLAB (The MathworksTM Inc.). It is needed to mention the speed of the processor we used here for analysis as processing time can vary widely with the change of the processing speed of the processor. The intricate mathematics of the 2D TPS process is not the concern; MATLAB has separate toolboxes e.g., *Curve fitting toolbox* and *Spline toolbox* are used to apply TPS interpolation on the data which eventually generates the interpolated data table.

4. RESULTS

In the following sections improvement of the various performance parameters after will be shown (after applying TPS):

4.1 Comparison of the variation SNR_e and CNR_e with respect to the strain

SNR_e depicts the most crucial sketch of the quality of the strain images as it is actually related to the signal quality itself which is taken after the post compression. In research methodology to prove a fact we sometimes compare the experimental result of the proposed method with already established algorithm. In our case we have chosen 'Simple Smooth Spline (1D)' and the 'Adaptive Stretching' as our comparing parameters to analyze our proposed 2D thin plate smoothing spline method. It is quite understandable from the figure-3 that though at lower strain 2D plate spline method giving a much better SNR_e compared with the other two; but at the higher strain performance of the simple spline worth mentioning. Though effectiveness of the 2D smoothing spline method is applicable for the lower percentage strain; it can be a promising technique while it is needed to deal only with less percentage applied strain. Figure-4 depicts

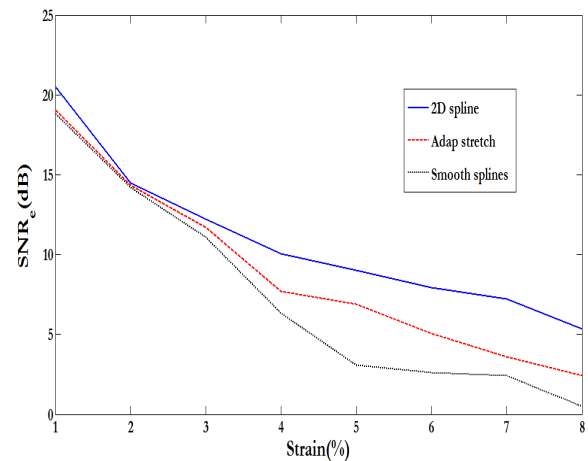


Fig. 3. Change of SNR_e with the variation of applied percentage strain(%).

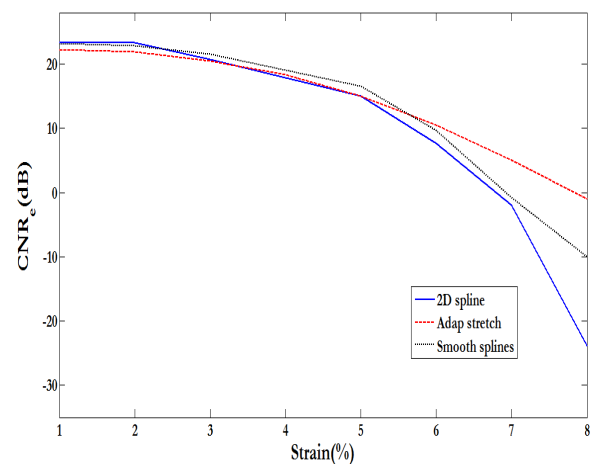


Fig. 4. Change of CNR_e with the variation of applied percentage strain(%).

the change of CNR_e with the variation of applied percentage strain(%).

4.2 Effect of smoothing parameter on SNR_e and CNR_e

In the whole process smoothing parameter, definitely plays an important role which controls the smoothness in other words best approximation of the displacement values. Over smoothness may lead to an elastogram which could be misleading. For a specific smoothing parameter which is used for both the dimensions we will get a specific point in the graph of the SNR_e and CNR_e vs smoothing parameter [28]. After constructing the graphs we can find an optimum value of ρ . Figure 5 & 6 we can see that SNR_e and CNR_e behave differently with the increase of smoothing parameter (ρ). Analyzing equation-1 ρ is multiplied with the first part where in the second part $(1-\rho)$ is multiplied. Therefore we are unable to reach a conclusion about any linear relationship. Both the figures plotted considering smoothing parameter also reflects the fact identified.

4.3 Change in CNR_e and SNR_e with the variation of weight parameter

According to the mathematical description what we have mentioned earlier in equation-1 there is option to vary the weight pa-

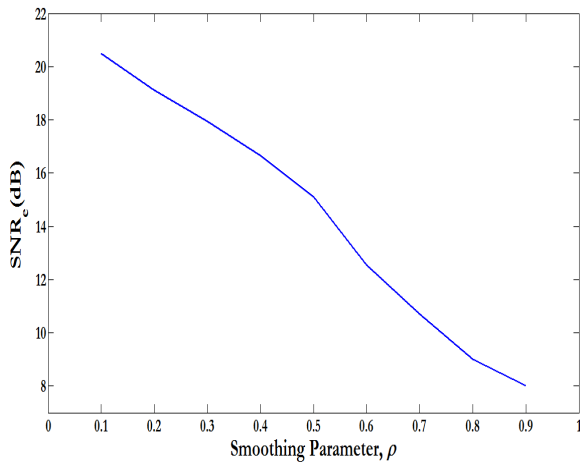


Fig. 5. Variation of SNR_e with smoothing parameter (ρ).

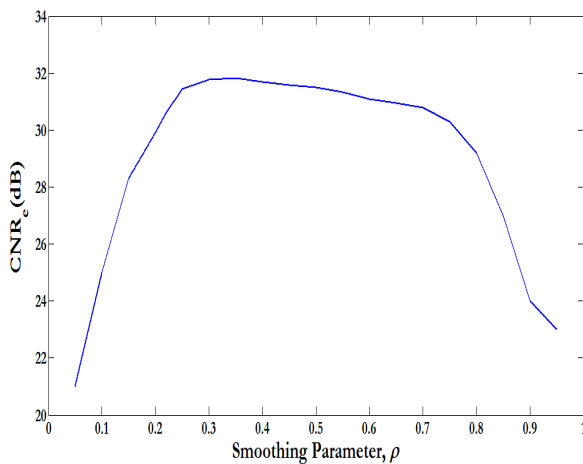


Fig. 6. Variation of CNR_e with smoothing parameter (ρ).

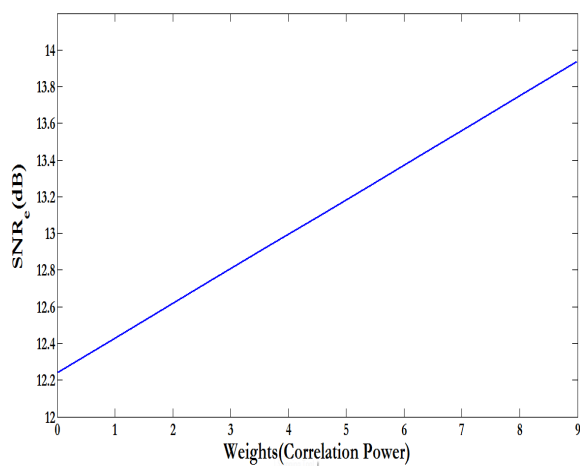


Fig. 7. Variation of SNR_e with the increase of weights (w_i).

parameter which is expressed as w_i and varying that we will give attention to the variation of SNR_e and CNR_e . If we define 'c' as the correlation value corresponding to the displacement estimate then w_i is expressed as $w_i=c_i$ where $i = 0,1,2,3,4,5\dots$ and so on. We know for displacement estimate we need time delay estimation and for that correlation technique is necessary. Figure 7 & 8 shows the change of SNR_e and CNR_e with the increase of w_i and

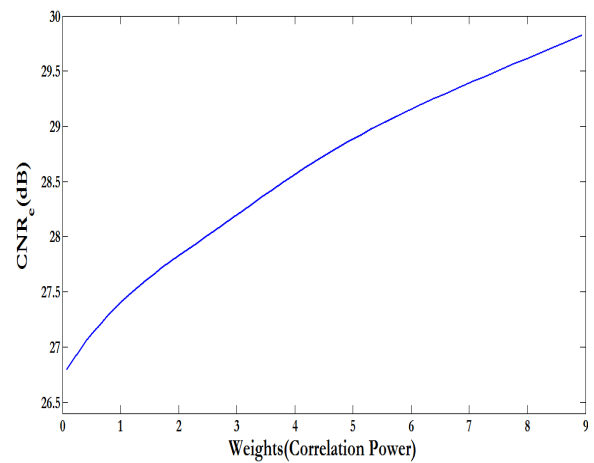


Fig. 8. Variation of CNR_e with the increase of weights (w_i).

both of them increase in each cases. SNR_e increases with a complete linearity with the increase of weights (correlation power). But from figure-8 we can see CNR_e (dB) is 26.8 dB near the zero correlation power value. Then increases almost linearly.

4.4 Variation of percentage strain with step increase or decrease

We will use step increase or decrease as an analytical parameter to observe the robustness of 2D plate smoothing spline method

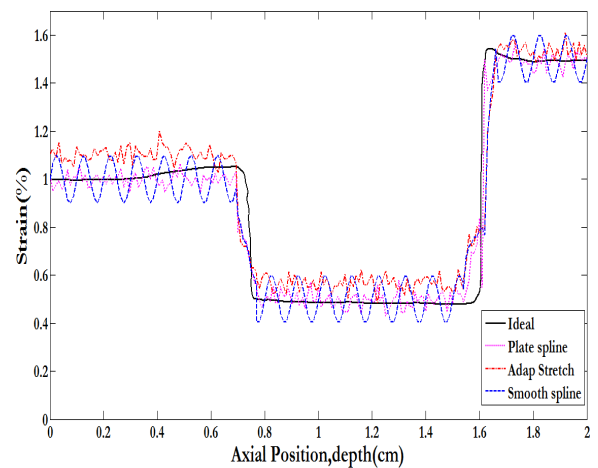


Fig. 9. Percentage Strain (%) vs. Axial position (cm) with step input applied.

compared to other techniques. Experimenting with the the step response the main concerning points are the rise-time and fall-time. Faster rise-time and fall-time are related to the resolution which is one of the unavoidable performance parameter for measuring the overall quality of a strain image. Adaptive Stretching performs most promisingly having the fastest rise and fall time. It is noticeable that the average following score of 2D spline method to follow the ideal one is better than the simple plate spline technique. As we need taking into account both dimensions axial and lateral in our method. But the process is complex and vulnerable to noise to apply Adaptive Stretching and simple plate spline in lateral direction. So in the figure-9 of lateral distance (depth, cm scale) vs. percentage strain we just focused on comparing step responses changing the smoothing parameters. It is clear from figure-10 that smoothing parameter, $\rho = 0.6$

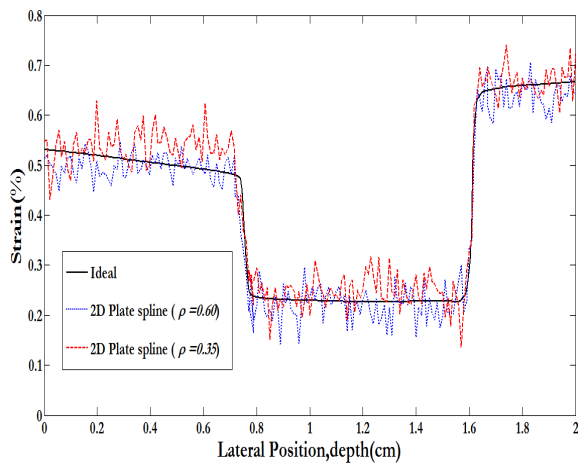


Fig. 10. Percentage Strain(%) vs. Lateral position (cm) with step input applied.

is more successful compared to $\rho = 0.35$ in case of increasing elastographic resolution.

5. VISUAL PERFORMANCE COMPARISONS OF THE STRAIN IMAGES ACQUIRED BY SEVERAL TECHNIQUES

Figure-11 gives us a comparative idea regarding the performance of the 2D plate smoothing spline estimator with the 1D spline the adaptive stretching method. In practical (clinical) use of the whole elastographic method primary target is to have a visually eased elastograms where artifacts are potentially reduced and accurate detection & identification of undesired hard nodule is feasible [11]. We have applied percentage strain of 1%, 2%, 4% and 8%. We used a standard window length of 2mm and window overlap of 2mm, which is actually same as the window length. We have applied the strain operation on the displacement values and after the smoothing operation we've taken the gradient operation finally. Median filtering was done to make the elastograms smoother. With the lower applied strain they are showing a better result in comparison with the result at higher applied strain. Higher strain caused unwanted noise and thus as a resultant effect there is introduction of the artifacts degrading the comprehensibility of the malignant targeted lesions with its background. The entire experimentation with our proposed technique of the 2D spline is quite satisfactory compared with the smoothing spline method. But it should be mentioned about the unavoidable trade-off related with this is the manipulation and the calculation time.

6. CONCLUSION

It is essential for any scientific research to have improved performance. But most of the times that comes with a time consuming mathematical model. Our world is experiencing a rapid boom in computing technology which is dedicated to curb provide processing time for the Our world is experiencing a rapid boom in computing technology which is dedicated to reduce processing time for the digital electronic devices. In practical cases when an actual ultrasonic probe will be used there will be always some undesired motion which can not be ignored [29] [30] [31]. So a robust strain estimator which can provide more efficient immunity from noise could be remarkable.

2D spline might be one way to reduce the noise. To locate a malignant area with a finer accuracy we need to take into account all the directions axial, lateral and elevational. But with freehand

scanning there are so many limitations mainly uniform scanning of the portion is not feasible [32]. Here we need more sophisticated setup of the whole ultrasound scanning system which is fully automated by the use of computers. A special design of the ultrasound transducer is also necessary. If we can take in to account all the dimension axial, lateral and elevational and then apply 2D spline with pairs, after that superimposition of all the combinations are expected to produce better results. In 3D implementation we need to find and fix a steady smoothing parameter where elastographic resolution is high and calculation time is also efficient. Parallel Computing using Graphics Processing Unit (*GPU*) could be used as a pragmatic solution for applying 2D spline method in clinical setup [33] [34].

7. ACKNOWLEDGEMENTS

Heartfelt thanks to Dr. S. Kaisar Alam who is working as a member of the research staff at *Lizzi Center for Bio-medical Engineering of Riverside Research Institute (NY, USA)* for his contribution by providing necessary resources to conduct this research work.

The author also likes to thank Niamul Quader, PhD student at *University of British Columbia (UBC), Vancouver, CA* for his useful support and suggestions throughout the entire process.

8. REFERENCES

- [1] Ophir, J., I. Cespedes, Ponnekanti, H., Yazdi, Y., & Li, X. "Elastography: a quantitative method for imaging the elasticity of biological tissues." *Ultrasonic imaging*, 13(2), 111-134, 1991.
- [2] Yeh, W. C., Li, P. C., Jeng, Y. M., Hsu, H. C., Kuo, P. L., Li, M. L., & Lee, P. H. "Elastic modulus measurements of human liver and correlation with pathology." *Ultrasound in medicine & biology*, 28(4), 467-474, 2002.
- [3] Greenleaf, J. F., Fatemi, M., & Insana, M. "Selected methods for imaging elastic properties of biological tissues. Annual review of biomedical engineering, 5(1), 57-78, 2003.
- [4] Fung, Y. C., & S. C. Cowin. "Biomechanics: Mechanical properties of living tissues." *Journal of Applied Mechanics*, 61(4), 1007-1007, 1994.
- [5] Turgay, E., Salcudean, S., & Rohling, R. "Identifying the mechanical properties of tissue by ultrasound strain imaging." *Ultrasound in medicine & biology*, 32(2), 221-235, 2006.
- [6] O'Donnell, M., Emelianov, S. Y., Skovoroda, A. R., Lubinski, M. A., Weitzel, W. F., & Wiggins, R. C. "Quantitative elasticity imaging." In *Ultrasonics Symposium, Proceedings.*, IEEE, 893-903, 1993.
- [7] Righetti, R., Ophir, J., & Ktonas, P. "Axial resolution in elastography." *Ultrasound in medicine & biology*, 28(1), 101-113, 2002.
- [8] Thangavel, K., Manavalan, R., & Aroquiaraj, I. L. "Removal of speckle noise from ultrasound medical image based on special filters: comparative study." *ICGST-GVIP Journal*, 9(3), 25-32, 2009.
- [9] Alam, S. K. "Novel spline-based approach for robust strain estimation in elastography." *Ultrasonic imaging*, 32(2), 91-102, 2010.
- [10] Khadem, A., & Setarehdan, S. K. "Smoothing-Spline based Strain Estimation in Ultrasound Elastography." In *Proc. IEEE International Conference on Signal Processing and Communications, (ICSPC)*, 680-683, IEEE, November 2007.
- [11] Hakim, S. B., & Islam, K.K. "A Comparative Analysis of Processing Periods for Strain Images generated using 1D Spline based approach and 2D Thin Plate Smoothing Spline method." *International Conference on Informatics, Electronics & Vision (ICIEV)*, IEEE, 1-6, May 2013.

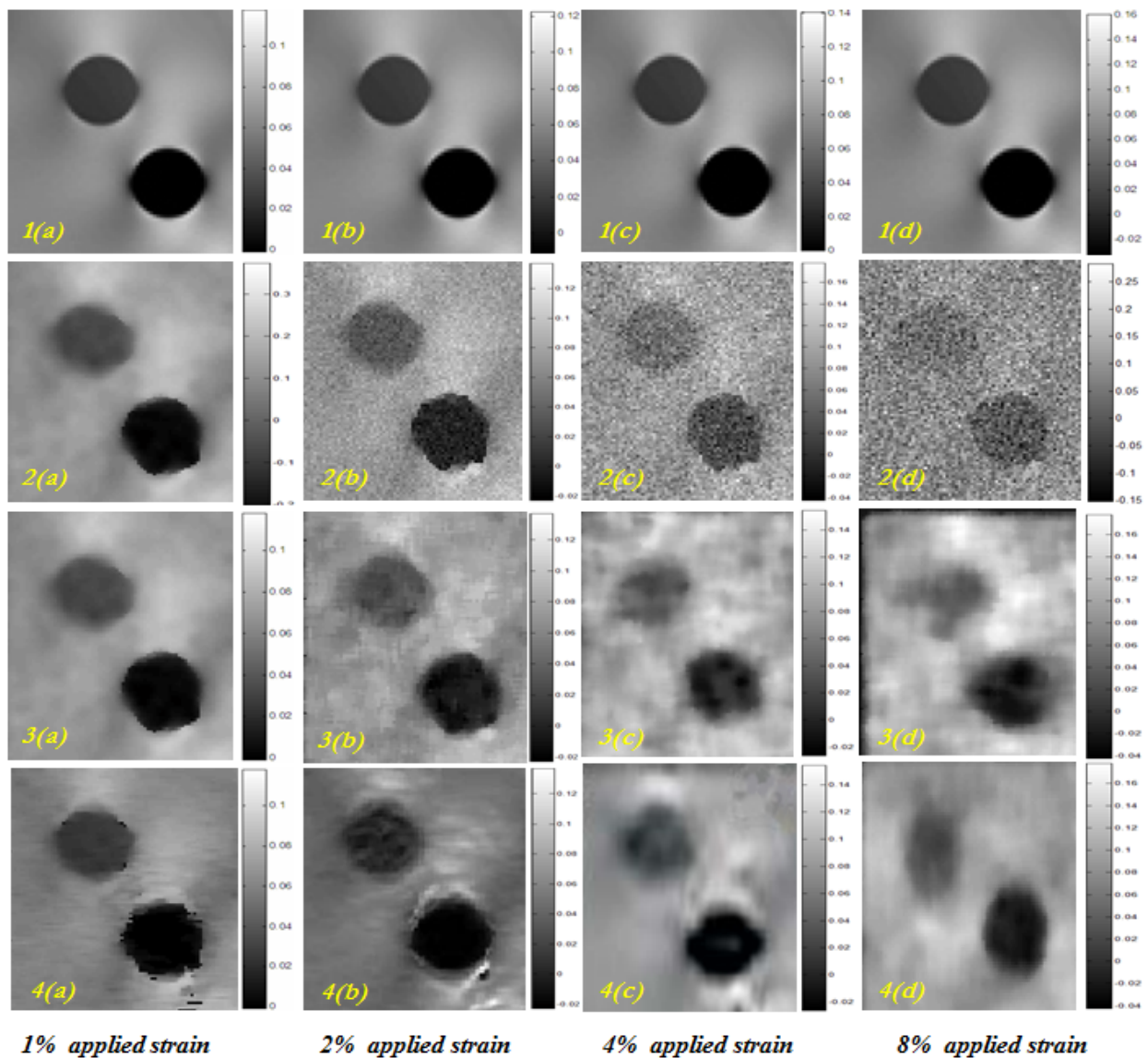


Fig. 11. Strain images of the FEM simulation phantom generated by different method, Results 1(a) to 1(d) is taken as ideal (simulated) in varied applied strain, Results 2(a) to 2(d) is generated by Smooth Spline method, Results 3(a) to 3(d) is generated by Adaptive stretching method, Results 4(a) to 4(d) is generated by 2D plate smoothing Spline method.

[12] Srinivasan, S., Righetti, R., & Ophir, J. "Trade-offs between the axial resolution and the signal-to-noise ratio in elastography." *Ultrasound in medicine & biology*, 29(6), 847-866, 2003.

[13] Varghese, T., & Ophir, J. "A theoretical framework for performance characterization of elastography: The strain filter." *IEEE Transactions on Ultrasonics, Ferroelectrics and Frequency Control*, 44(1), 164-172, 1997.

[14] Kallel, F., & Ophir, J. "A least-squares strain estimator for elastography." *Ultrasonic imaging*, 19(3), 195-208, 1997.

[15] Alam, S. K., Ophir, J., & Konofagou, E. E. "An adaptive strain estimator for elastography." *IEEE Transactions on Ultrasonics, Ferroelectrics and Frequency Control*, 45(2), 461-472, 1998.

[16] Buckley, M. J. "Fast computation of a discretized thin-plate smoothing spline for image data." *Biometrika*, 81(2), 247-258, 1994.

[17] Craven, P., & Wahba, G. "Smoothing noisy data with spline functions." *Numerische Mathematik*, 31(4), 377-403, 1978.

[18] Franke, R. "Smooth interpolation of scattered data by local thin plate splines." *Computers & Mathematics with Applications*, 8(4), 273-281, 1982.

[19] Gervini, D. "Free-knot spline smoothing for functional data." *Journal of the Royal Statistical Society: Series B (Statistical Methodology)*, 68(4), 671-687, 2006.

[20] Viola, F., & Walker, W. F. "A spline-based algorithm for continuous time-delay estimation using sampled data." *IEEE Transactions on Ultrasonics, Ferroelectrics and Frequency Control*, 52(1), 80-93, 2005.

[21] Ophir, J., Alam, S. K., Garra, B., Kallel, F., Konofagou, E., Krouskop, T., & Varghese, T. "Elastography: ultrasonic estimation and imaging of the elastic properties of tissues." *Proceedings of the Institution of Mechanical Engineers, Part H: Journal of Engineering in Medicine*, 213(3), 203-233, 1999.

[22] Sibson, R., & Stone, G. "Computation of thin-plate splines." *SIAM Journal on Scientific and Statistical Computing*, 12(6), 1304-1313, 1991.

- [23] Taghvakish, S., & Amini, J. "Optimum Weight in Thin Plate Spline for Digital Surface Model Generation." FIG Working Week (2004). TS26 Positioning and Measurement Technologies and Practices II. Athens, Greece, May : 22-27, 2004.
- [24] Bazen, A. M., & Gerez, S. H. "Fingerprint matching by thin-plate spline modelling of elastic deformations." Pattern Recognition, 36(8), 1859-1867, 2003.
- [25] Rohr, K., Stiehl, H. S., Sprengel, R., Buzug, T. M., Weese, J., & Kuhn, M. H. "Landmark-based elastic registration using approximating thin-plate splines." IEEE Transactions on Medical Imaging, 20(6), 526-534, 2001.
- [26] Krouskop, T. A., Wheeler, T. M., Kallel, F., Garra, B. S., & Hall, T. "Elastic moduli of breast and prostate tissues under compression." Ultrasonic imaging, 20(4), 260-274, 1998.
- [27] Samani, A., Zubovits, J., & Plewes, D. "Elastic moduli of normal and pathological human breast tissues: an inversion-technique-based investigation of 169 samples." Physics in medicine & biology, 52(6), 1565, 2007.
- [28] Wahba, G. "A comparison of GCV and GML for choosing the smoothing parameter in the generalized spline smoothing problem." The Annals of Statistics, 1378-1402, 1985.
- [29] Chandrasekhar, R., Ophir, J., Krouskop, T., & Ophir, K. "Elastographic image quality vs. tissue motion in vivo." Ultrasound in medicine & biology, 32(6), 847-855, 2006.
- [30] Barry, C. D., Allott, C. P., John, N. W., Mellor, P. M., Arundel, P. A., Thomson, D. S., & Waterton, J. C. "Three-dimensional freehand ultrasound: image reconstruction and volume analysis." Ultrasound in medicine & biology, 23(8), 1209-1224, 1997.
- [31] Xiao, G., Brady, J. M., Noble, J. A., Burcher, M., & English, R. "Nonrigid registration of 3-D free-hand ultrasound images of the breast." IEEE Transactions on Medical Imaging, 21(4), 405-412, 2002.
- [32] Souchon, R., Soualmi, L., Bertrand, M., Chapelon, J. Y., Kallel, F., & Ophir, J. "Ultrasonic elastography using sector scan imaging and a radial compression." Ultrasonics, 40(1), 867-871, 2002.
- [33] Montagnon, E., Hissoiny, S., Desprs, P., & Cloutier, G. "Real-time processing in dynamic ultrasound elastography: A GPU-based implementation using CUDA." 11th International Conference on Information Science, Signal Processing and their Applications (ISSPA), IEEE, 472-477, July 2012.
- [34] Deshmukh, N., Rivaz, H., & Boctor, E. "GPU-based elasticity imaging algorithms." In Proc. International Conference on Medical Image Computing and Computer Assisted Intervention, 2009.

About the Authors :

Safayat Bin Hakim completed his undergraduate in Electrical and Electronic Engineering (EEE) from Islamic University of Technology (IUT).

Dr. Kazi Khairul Islam working as a professor in the Department of EEE at Islamic University of Technology (IUT).